Antarctic Science 29(3), 217–228 (2017) © Antarctic Science Ltd 2017 doi:10.1017/S0954102016000699

Short timescale dynamics of phytoplankton in Fildes Bay, Antarctica

CLAUDIA EGAS[1], CARLOS HENRÍQUEZ-CASTILLO[1,2,3], NATHALIE DELHERBE[2], ERNESTO MOLINA[4], ADRIANA LOPES DOS SANTOS[5], PARIS LAVIN[6], RODRIGO DE LA IGLESIA[1,3], DANIEL VAULOT[5] and NICOLE TREFAULT[7]

[1]*Departamento de Genética Molecular y Microbiología. Facultad de Ciencias Biológicas, Pontificia Universidad Católica de Chile, Portugal 49, Santiago, Chile*
[2]*Laboratorio de Oceanografía Microbiana, Departamento de Oceanografía, Universidad de Concepción, PO Box 160-C, Concepción, Chile*
[3]*Instituto Milenio de Oceanografía, Universidad de Concepción, Concepción, Chile*
[4]*Departamento de Ecología, Facultad de Ciencias Biológicas, Pontificia Universidad Católica de Chile, Portugal 49, Santiago, Chile*
[5]*Sorbonne Universités, UPMC Université Paris 06, CNRS, UMR7144, Station Biologique, Place Georges Teissier 29680, Roscoff, France*
[6]*Laboratorio de Complejidad Microbiana y Ecología Funcional, Instituto Antofagasta, Universidad de Antofagasta, Avenida Angamos 601, Antofagasta, Chile*
[7]*Centro de Genómica y Bioinformática, Facultad de Ciencias, Universidad Mayor, Camino La Pirámide 5750, Huechuraba, Santiago, Chile*
nicole.trefault@umayor.cl

Abstract: Phytoplankton is responsible for most primary production in Antarctica, but the short timescale dynamics of its size structure and composition are poorly described and understood. The abundance and composition of phytoplankton in Fildes Bay, western Antarctic Peninsula, was followed for 12 days during the summer using a range of methods, including size fractionation of chlorophyll, microscopy, flow cytometry and terminal-restriction fragment length polymorphism (T-RFLP) of the plastid 16S rRNA gene. A rapid increase in biomass and cell abundance occurred in response to a vertical mixing event. This increase also resulted in a shift in composition from diatoms to Prymnesiophyceae, and then back to diatoms as the water column re-stratified. Our results show a strong dominance of nanophytoplankton represented by *Thalassiosira* and *Phaeocystis*. The rapid response of the phytoplankton suggests that it is well adapted to short-term environmental changes.

Received 1 May 2016, accepted 18 October 2016, first published online 31 January 2017

Key words: Antarctic marine microorganisms, microbial photosynthetic eukaryotes, molecular fingerprinting, phytoplankton size structure

Introduction

Antarctic waters constitute very productive areas of the world's oceans on a short-term basis (Arrigo *et al.* 1998) with photosynthetic eukaryotes being the major group responsible for primary production. Antarctic productivity is high during the summer, when ice melts and light levels are elevated, and declines to near zero during the long winter. Phytoplankton standing stocks in these waters are thought to be influenced mostly by water column stability, since most micro- and macronutrients have been shown to be abundant (Vernet *et al.* 2008). Freshwater input from sea ice and glaciers plays a critical role in water column stratification and light penetration, affecting phytoplankton photosynthesis, especially in coastal environments (Vernet *et al.* 2008, Gonçalves-Araujo *et al.* 2015).

The western Antarctic Peninsula (WAP) has shown important decadal temperature changes not primarily associated with global temperature change drivers (Turner *et al.* 2016). Environmental shifts within the WAP have resulted in changes in biomass and composition of primary producers (Montes-Hugo *et al.* 2009, Gonçalves-Araujo *et al.* 2015). However, the short timescale dynamics of phytoplankton size structure and the taxonomic identity of the main representatives are not well known. In the WAP, surface waters are mostly dominated by pico- and nanoplankton (0.2–3 µm and 3–20 µm, respectively) (Garibotti *et al.* 2003, Montes-Hugo *et al.* 2008, Lee *et al.* 2015). However, occasional blooms of microphytoplankton (20–200 µm) contribute considerably to the high primary production and biomass observed in summer (Moline *et al.* 1997, Clarke *et al.* 2008, Schloss *et al.* 2012). In these waters, picophytoplankton is dominated by prasinophytes and haptophytes (Agawin *et al.* 2002, Gonçalves-Araujo *et al.* 2015), while cryptophytes and small diatoms dominate the nanophytoplankton (Garibotti *et al.* 2005). Diatoms and dinoflagellates, from the *Thalassiosira*, *Fragilariopsis* and *Heterocapsa* genera, are mostly found in the microplankton (Piquet *et al.* 2008, Gonçalves-Araujo *et al.* 2015, Pearson *et al.* 2015).

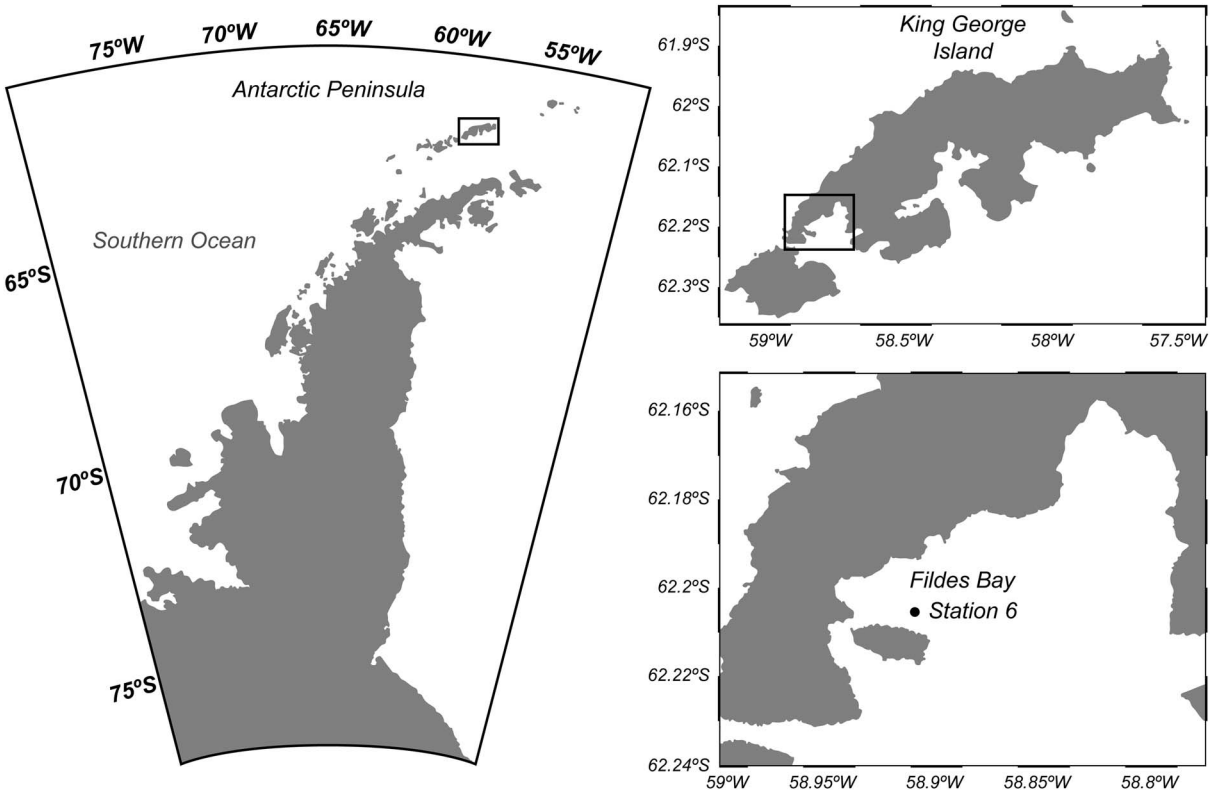

Fig. 1. Location of the sampling area in Fildes Bay, King George Island, Antarctica.

Fildes Bay (King George Island) is located at the north-western tip of the WAP. In this coastal region, Lee *et al.* (2015) estimated the average contribution of pico- and nanophytoplankton between 1996 and 2008 to be 63% of the total chl *a* and 86% of cell abundance. Molecular diversity and community composition analyses using high-throughput sequencing of the 18S rRNA gene for the $< 20\,\mu m$ size fraction indicated that the dominant taxa belonged to dinoflagellates, cryptophytes, prymnesiophytes, diatoms and chlorophytes (Luo *et al.* 2015). More recently,

Table I. Sampling date, depth, and environmental and cell abundance data.

Sample	Depth (m)	Date	Temperature (°C)	Salinity	PAR (μmol photons m^{-2} s^{-1})	Cell abundance (10^3 cells ml^{-1}) PPE	PNE	CRY	Samples subjected to specific analyses Light microscopy	DNA (T-RFLP)
M11-1	5	4 Feb 2012	1.5	34.1	277.9	0.16	1.01	0.09	*	*
M11-2	26		1.1	34.1	35.5	0.34	0.69	0.22		*
M12-1	5	6 Feb 2012	2.1	33.8	309.6	1.48	7.27	1.30		
M12-2	20		1.5	34.1	39.6	0.76	2.61	0.59		
M13-1	5	7 Feb 2012	2.1	34.0	646.4	1.11	5.15	0.92		*
M13-2	15		1.6	34.1	90.4	1.71	6.03	1.66	*	*
M14-1	5	8 Feb 2012	n.a.	n.a.	n.a.	1.27	6.80	0.78	*	
M14-2	19		n.a.	n.a.	n.a.	1.26	4.98	1.17	*	
M15-1	5	9 Feb 2012	n.a.	n.a.	n.a.	1.14	3.05	0.91	*	
M15-2	18		n.a.	n.a.	n.a.	1.29	3.64	1.06	*	
M16-1	5	11 Feb 2012	1.6	34.1	67.9	1.47	4.03	1.02		*
M16-2	15		1.6	34.1	18.2	1.04	3.40	0.90		*
M17-1	5	13 Feb 2012	2.4	33.9	352.3	1.34	5.00	0.86	*	
M17-2	10		1.9	34.0	43.1	1.16	5.44	0.59	*	
M18-1	5	15 Feb 2012	2.0	33.9	144.4	1.61	7.10	0.61	*	
M18-2	9		2.0	33.9	25.7	1.49	7.84	1.04	*	

CRY = cryptophytes, n.a. = not available, PAR = photosynthetic active radiation, PNE = photosynthetic nanoeukaryotes, PPE = photosynthetic picoeukaryotes, T-RFLP = terminal-restriction fragment length polymorphism.

https://doi.org/10.1017/S0954102016000699 Published online by Cambridge University Press

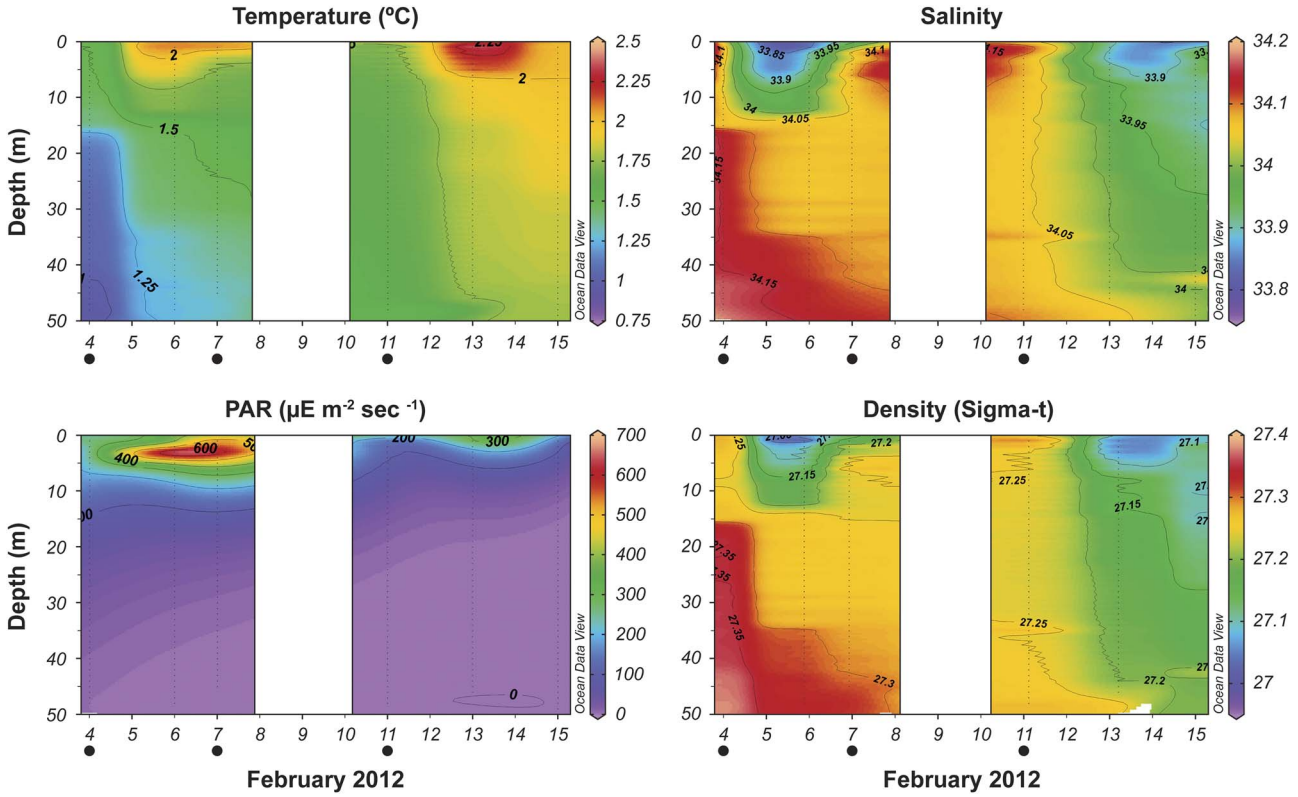

Fig. 2. Temporal variation of physicochemical parameters (temperature, salinity, photosynthetic active radiation (PAR) and density) in Fildes Bay, King George Island. Filled circles below the x-axis represent the days when DNA samples were collected.

Moreno-Pino *et al.* (2016), using high-throughput sequencing of the 16S rRNA plastidial gene, showed that these waters are dominated by diatoms, haptophytes and cryptophytes.

Different methodological approaches have been used to characterize phytoplankton dynamics in Antarctic coastal waters. Most studies have relied on chl *a* and microscopic observations (Wright *et al.* 2009, Lee *et al.* 2015). Flow cytometry has also been used to determine the abundance of different photosynthetic populations in Antarctic waters (Boyd *et al.* 2000, Díez *et al.* 2004). Molecular fingerprinting techniques, such as denaturing gradient gel electrophoresis (DGGE) and terminal-restriction fragment length polymorphism (T-FRLP), have allowed the rapid characterization of phytoplankton composition (Baldwin *et al.* 2005, Piquet *et al.* 2008). Traditionally, these fingerprinting techniques have used the 18S rRNA gene, which targets all eukaryotes. The use of the plastidial 16S rRNA gene greatly enhances the specificity of these approaches, since it selectively targets photosynthetic groups (Henríquez-Castillo *et al.* 2015, Moreno-Pino *et al.* 2016).

Here, the hypothesis that Antarctic phytoplankton experiences rapid changes in response to water column conditions over short timescales was tested. The phytoplankton dynamics in Fildes Bay were examined over 12 days in February 2012 using size fractionation of chl *a*, microscopy, flow cytometry and T-RFLP of the plastidial 16S rRNA gene. Our data reveal a dramatic change in phytoplankton biomass and composition following a water column mixing event.

Methods

Study site and sampling

Seawater samples were collected in Fildes Bay, King George Island, at Station 6 (62°12'11"S, 58°55'15"W) using 51 Niskin bottles on eight different days between 4–15 February 2012 (Fig. 1 and Table I). Samples were taken near the surface (5 m) and at a depth corresponding to 10% of the surface photosynthetic active radiation (PAR) (9–26 m, Table I). Samples were prefiltered on board through a 100 µm mesh, stored in sterile plastic carboys and kept in darkness until further processing. Once at the laboratory (< 2 h later), subsamples for chl *a*, flow cytometry, microscopy and molecular analyses were taken.

Physicochemical parameters

Temperature (SST), salinity and PAR measurements were obtained using a CTD SBE 911 plus (SeaBird Electronics) equipped with an auxiliary biospherical PAR sensor

https://doi.org/10.1017/S0954102016000699 Published online by Cambridge University Press

(LiCor LI-193). The CTD casts were processed and validated with the SBE data processing software version 7.23.2.

Chlorophyll determination

Total and fractionated chl *a* were determined from triplicate 100 ml subsamples. For total chl *a*, biomass (< 100 µm) was collected on 25 mm diameter GF/F filters (Whatman). For fractionated chl *a*, seawater samples were filtered through 20 µm (Nylon, Millipore) and 3 µm (Polycarbonate, Millipore) pore size filters. The biomass recovered from each fraction was collected on 25 mm diameter GF/F filters (Whatman) to obtain chl *a* < 20 µm and chl *a* < 3 µm, respectively. Filtration was completed in the dark immediately after the samples arrived to the laboratory. Chlorophyll *a* and pheopigments were determined by fluorometry. Pigments were extracted in 90% acetone for 24 h at -20°C and analysed on a Turner Designs Trilogy fluorometer, according to the method of Holm-Hansen *et al.* (1965). Calibration was made with a chl *a* standard (Sigma-Aldrich).

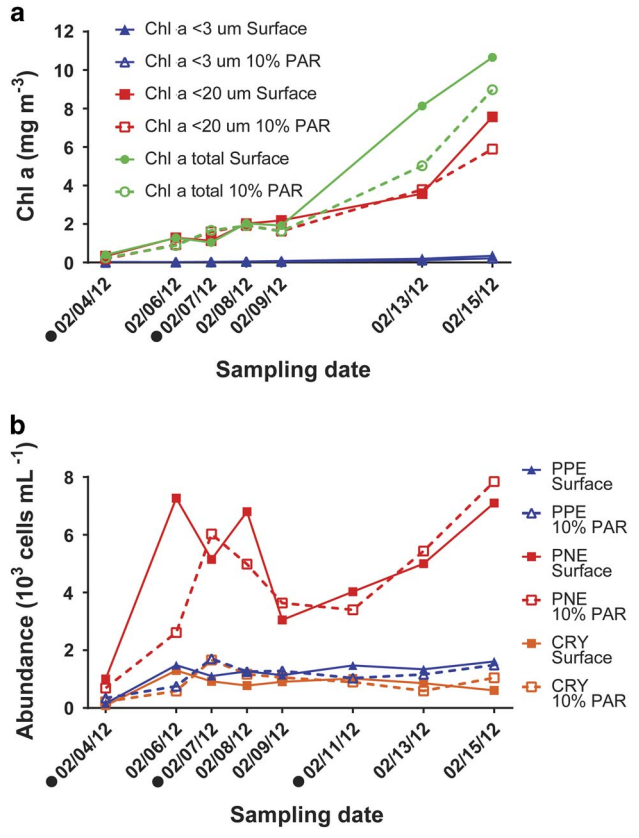

Fig. 3a. Chlorophyll *a* and **b.** phytoplankton abundance during the sampling period. Filled symbols correspond to surface samples and open symbols to 10% photosynthetic active radiation (PAR) samples. Filled circles below the x-axis represent the days when DNA samples were collected. CRY = cryptophytes, PNE = nanoeukaryotes, PPE = picoeukaryotes.

Abundance of photosynthetic eukaryotes by flow cytometry

Subsamples of 1.35 ml were taken in triplicates, fixed with 150 µl of fixative (1% paraformaldehyde, 0.5% glutaraldehyde, 100 mM sodium borate, pH 8.4), incubated for 20 min at room temperature and fast frozen in liquid nitrogen. Photosynthetic eukaryote abundances were enumerated with a 'jet-in-air' influx flow cytometer (Becton Dickinson) using blue 488 nm and red 640 nm lasers. Particles were differentiated by forward angle light scatter and trigger pulse width from the 488 nm laser, and red fluorescence (692/40 nm) detection from the 488 and 640 nm lasers. Fluorescent Ultra Rainbow Beads (3 µm, Spherotech) were used for calibration. Each sample was run at an average flow rate of 47 µl min^{-1} for 5 min. Analyses were performed with the FlowJo software (Tree Star).

Abundance of microplankton by light microscopy

Duplicate 50 ml seawater subsamples were taken every day and fixed with 1% formaldehyde and counted using the Utermöhl's method (Hasle 1978). The microplankton was counted at 400x in 15 random fields or by counting cells throughout the whole settling chamber, depending on the density of cells, under phase contrast microscopy

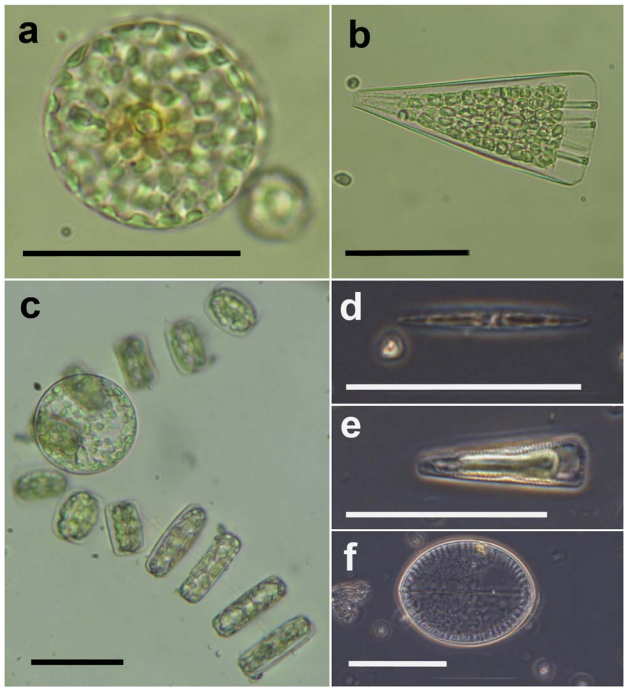

Fig. 4. Phase contrast light microscopy of microphytoplankton. Scale bars represent 50 µm. **a.** Centric planktonic diatom *Thalassiosira* sp. valve view. **b.** Pennate epiphytic diatom *Licmophora* sp. cell in girdle view, separated from a colony. **c.** Colonies of the centric planktonic diatom *Thalassiosira* sp. in girdle view. **d.** Pennate planktonic diatom *Nitzschia* sp. **e.** Pennate diatom. **f.** Pennate planktonic diatom *Cocconeis* sp.

https://doi.org/10.1017/S0954102016000699 Published online by Cambridge University Press

using a Nikon Eclipse T100 microscope. All organisms with a length > 20 µm were counted.

DNA extraction

Samples of 4.5 l of seawater were size fractionated using a peristaltic pump (Cole-Palmer) by sequential filtration using 47 mm diameter Swinnex filter holder (Millipore), and 60 µm, 20 µm (Nylon, Millipore), 12 µm, 3 µm and 0.2 µm (Polycarbonate, Millipore) pore size filters. Filters were stored in 2 ml cryovials at -196°C or -80°C until analysis. All steps were performed under sterile conditions. Filters were thawed and half of the filters were cut into small pieces, while the other half was kept at -20°C as backup. Each half-filter was incubated in lysis buffer (TE 1x/NaCl 0.15 M), with 10% SDS and 20 mg ml^{-1} proteinase K at 37°C for 1 h. DNA was extracted using 5 M NaCl and hexadecyl-trimethyl-ammonium bromide (CTAB) extraction buffer (10% CTAB, 0.7% NaCl) and incubated at 65°C for 10 min before protein removal using a conventional phenol-chloroform method. DNA was precipitated using ethanol at -20°C for 1 h and resuspended in 50 µl Milli-Q water (Millipore). DNA integrity was evaluated by agarose gel electrophoresis and quantified using a fluorometric assay (Qubit 2.0 fluorometer).

Terminal-restriction fragment length polymorphism

Phytoplankton composition was determined by T-RFLP analysis for three sampling days: 4, 7 and 11 February (see Table I). The plastid 16S rRNA gene was amplified by polymerase chain reaction (PCR) with plastidial biased primers PLA491F (Fuller *et al*. 2006), labelled at the 5' end with the fluorochrome NED, and OXY1313R (West *et al*. 2001). The PCR mixture (25 µl final volume) contained 1.2 mM $MgCl_2$, 1X buffer, 0.2 mM dNTPs, 0.75 mM of each primer, 2.5 U KAPA Taq polymerase and 15–40 ng $µl^{-1}$ of DNA. The amplification conditions included one step at 94°C for 5 min, 30 cycles of 95°C for 30 sec, 60°C for 45 sec and 72°C for 1 min, and a final elongation at 72°C for 6 min.

Four restriction enzymes (*Hae*III, *Rsa*I, *Hha*I and *Alu*I) were tested to determine the one that best discriminates between the different phylotypes present in the samples. The labelled PCR products were digested independently with the four restriction enzymes. Restriction reactions comprised 2.5 U of restriction enzyme and 1X buffer (Promega) in a final volume of 20 µl at 37°C overnight. The restriction fragments were precipitated using 3 M sodium acetate and 100% v/v ice-cold ethanol (2.5 v) at -80°C for 1 h, centrifuged at 20 000 *g* at 4°C for 30 min, washed with 70% v/v ice-cold ethanol, again centrifuged at 20 000 *g* at 4°C for 30 min, air-dried and resuspended in a final volume of 20 µl of Milli-Q water (Millipore). The T-RFLP analyses were conducted at Macrogen, Seoul, using the internal size standard LIZ1200. Raw T-RFLP data were handled as previously described (Henríquez-Castillo *et al*. 2015). The average number of terminal-restriction fragments (T-RFs) obtained for *Hae*III, *Rsa*I, *Hha*I and *Alu*I were nine, ten, six and five, respectively. Since restriction enzymes *Hae*III and *Rsa*I appeared the most resolutive, all subsequent analyses were performed using only these two enzymes.

In silico *analysis of terminal-restriction fragments*

For taxonomic assignment of OTUs detected in the T-RFLP profiles, an *in silico* restriction analysis was performed, with the restriction enzymes *Hae*III and *Rsa*I, using Mothur software (Schloss *et al*. 2009). For this, sequences from major marine phytoplankton taxonomic groups (Dinophyceae, Cryptophyceae, Prasinophyceae, Prymnesiophyceae, Bacillariophyceae, Chlorophyceae, Mamiellophyceae) were retrieved from the PhytoREF database (Decelle *et al*. 2015), to which the 16S plastidial sequences previously obtained from Fildes Bay were added (GenBank KT964300-KT964307). After PLA491 primer alignment, restriction sites for the two enzymes

Table II. Abundance of microphytoplankton estimated by light microscopy.

Sample	Date	Abundance (ml^{-1})					
		Thalassiosira sp.	*Pseudo-nitzschia* sp.	*Prorocentrum antarcticum*	Pennate diatoms	Others	Total
M11-1	4 Feb 2012					1	1
M13-2	7 Feb 2012	1	2	11	27	12	52
M14-1	8 Feb 2012	1				1	2
M14-2	8 Feb 2012					1	1
M15-1	9 Feb 2012	2					2
M15-2	9 Feb 2012	1					1
M17-1	13 Feb 2012	369	17	3	7		396
M17-2	13 Feb 2012	508	4				512
M18-1	15 Feb 2012	88				3	91
M18-2	15 Feb 2012	72				67	139

https://doi.org/10.1017/S0954102016000699 Published online by Cambridge University Press

Table III. Taxonomic assignment of the *Hae*III terminal-restriction fragments (T-RFs).

*Hae*III T-RF	Mean relative abundance	SD	Class	Order	Family	Species	NCBI accession number	Other match representatives[a]	*Rsa*I T-RF[b]	Mean relative abundance	SD
173	0.04	0.17	N.A.								
245	6.46	7.66	N.A.								
252	2.39	3.85	Cryptophyceae	Pyrenomonadales	Geminigeraceae	*G. cryophila*	AB073111	*T. acuta*	401	8.9	9.3
			Cryptophyceae	Pyrenomonadales	Pyrenomonadaceae	*P. salina*	X55015				
			Cryptophyceae	Cryptomonadales	Cryptomonadaceae	*C. paramecium*	AF545624	*C. curvata*			
401	0.07	0.19	N.A.								
402	0.04	0.16	N.A.								
425	0.06	0.24	N.A.								
427	13.05	19.73	N.A.								
429	0.10	0.38	N.A.								
434	40.15	23.72	Prymnesiophyceae	Phaeocystales	Phaeocystaceae	*P. antarctica*	JN117275		396	19.8	12.1
			Prymnesiophyceae	Isochrysidales	Noelaerhabdaceae	*E. huxleyi*	NC_007288				
			Prymnesiophyceae	Isochrysidales	Isochrysidaceae	*Isochrysis* sp.	X75518				
440	23.12	33.95	Bacillariophyceae	Thalassiosirales	Thalassiosiraceae	*T. antarctica*	FJ002200	*T. punctigera, M. trioculatus*	836	38	28.5
			Bacillariophyceae	Thalassiosirales	Skeletonemataceae	*S. costatum*	X82154				
			Bacillariophyta		Phaeodactylaceae	*P. tricornutum*	FJ002225				
534	1.16	4.50	N.A.								
705	0.47	1.82	N.A.								
707	0.13	0.50	N.A.								
836	12.75	16.40	Mamiellophyceae	Mamiellales	Bathycoccaceae	*B. prasinos*	AY702131	*O. lucimarinus, M. squamata*	177	3.6	6.7

[a]Other representatives from the same taxonomic classification that match the T-RF size.
[b]Corresponds to the T-RF in the *Rsa*I profile.
N.A. = non-assigned, SD = standard deviation.
Taxonomic classification according to the PhytoREF database (July 2015).

were detected. Finally, the size of the *in silico* T-RF were compared with the observed T-RF. Taxonomic assignation was achieved i) with a ±2 nucleotides threshold and ii) checking for the presence of the peak of the taxon in both *Hae*III and *Alu*I restriction profiles.

Statistical analysis

Linear regression analyses were performed to test relationships between total and fractionated chl *a* using Prism 6.0 (GraphPad). The T-RFLP fingerprinting profiles were analysed using Primer 6 (Primer-E). Profiles were standardized and square root transformed. Starting with 92 T-RFLP$_{HaeIII}$ profiles obtained, an initial filter of those replicates not matching a 60% Bray–Curtis coefficient of similarity threshold, based on the relative abundances of each T-RFs, was applied. This filter reduced the total number of T-RFLP profiles to 55, which were used in further analyses (Table S1 found at http://dx.doi.org/10.1017/S0954102016000699). The resulting similarity matrix was used to obtain hierarchical cluster and non-metric multidimensional scaling (NMDS), for visual interpretation of the grouping and sorting of the data in a two-dimensional space. To evaluate statistically significant differences between size fractions, according to the relative abundances of taxonomic groups, analyses of similarity (ANOSIM) were performed based on the Bray–Curtis distance matrix. To explore the most important T-RFs for each group, SIMPER analysis were conducted. Spearman rank correlation analysis was performed to test the correlation between T-RFLP$_{HaeIII}$ and T-RFLP$_{RsaI}$ profiles using the Relate function in Primer 6 (Primer-E).

Results

Characterization of sampling site

Fildes Bay is a typical fjord-like Antarctic embayment located on King George Island (Fig. 1). In this bay, vertical profiles (down to 50 m) of temperature and salinity (Fig. 2) were measured over 12 days in February 2012. Temperature and salinity ranged from 1–2.25°C and 33.8–34.2, respectively. On 7 February, PAR surface maximum was 650 µmol photons m^{-2} sec^{-1}. A reduction in light penetration through the water column was observed during the sampling as evidenced by the decrease of 10% PAR depth, which was 26 m at the beginning of the sampling period *vs* 9 m at the end (Table I).

During the first two sampling days, 4 and 6 February, the water column was stratified with warmer waters at the surface. This was followed by a vertical mixing episode from 7–11 February (as shown in Fig. 2) that probably injected nutrients into the euphotic layer. Unfortunately, weather conditions between 7–11 February did not allow sampling. Afterwards, the water column tended to re-stratify with warmer surface waters until the last day of sampling when it mixed again.

Size fractionated chlorophyll a

Chlorophyll *a* levels were low at the beginning of the sampling period, with a steady increase after 6 February reaching > 10 mg m^{-3} chl *a* at the surface on the last day of sampling. Values for surface samples were higher than those from samples at 10% PAR (Fig. 3a). During the sampling period until 13 February, phytoplankton biomass in Fildes Bay was dominated by nanoplankton (Fig. 3b), with chl *a* < 20 µm accounting for 98% of total chl *a*. Nano- and picoplankton chl *a* were highly correlated with total chl *a* ($r^2 = 0.96$, $P = 0.0001$, $n = 7$ and $r^2 = 0.99$, $P < 0.0001$, $n = 7$, respectively). A sharp increase in total chl *a* was observed at the surface on 13 and 14 February, indicating a shift towards the microplankton size class (Fig. 3a).

Short timescale dynamics of phytoplankton abundance

Flow cytometry analysis indicated the presence of three major photosynthetic groups: picoeukaryotes (PPE), nanoeukaryotes (PNE) and a small group of phycoerythrin-containing nanoeukaryotes corresponding to cryptophytes (CRY). While the abundance of PPE and CRY was stable during the sampling period, with an average abundance of $1.2 \pm 0.4 \times 10^3$ and $0.8 \pm 0.4 \times 10^3$ ml^{-1}, respectively, PNE increased sharply after the first sampling day and remained three times more abundant than PPE and CRY thereafter (Fig. 3b).

Microscopic observations indicated the presence of different cell sizes of *Thalassiosira* sp., as well as *Pseudo-nitzschia* sp. and others species of pennate diatoms (Fig. 4 and Table II). These analyses showed a large increase of *Thalassiosira* sp. (> 20 µm) on 13 February in surface (sample M17) in concordance with the increase in total chl *a* (Fig. 3a and Table II). This event followed the mixing episode that took place between 7–11 February.

Photosynthetic eukaryotes: diversity and structure

Plastidial 16S rRNA gene fingerprints obtained from three sampling days: 4, 7 and 11 of February with the restriction enzymes *Hae*III and *Rsa*I (Tables S2 & S3 found at http://dx.doi.org/10.1017/S0954102016000699) showed a high correlation between the abundance matrices; therefore, only the results for *Hae*III are presented (Spearman rank correlation ρ: 0.8, $P < 0.0001$). From T-RFLP$_{HaeIII}$, six T-RFs accounted for > 90%

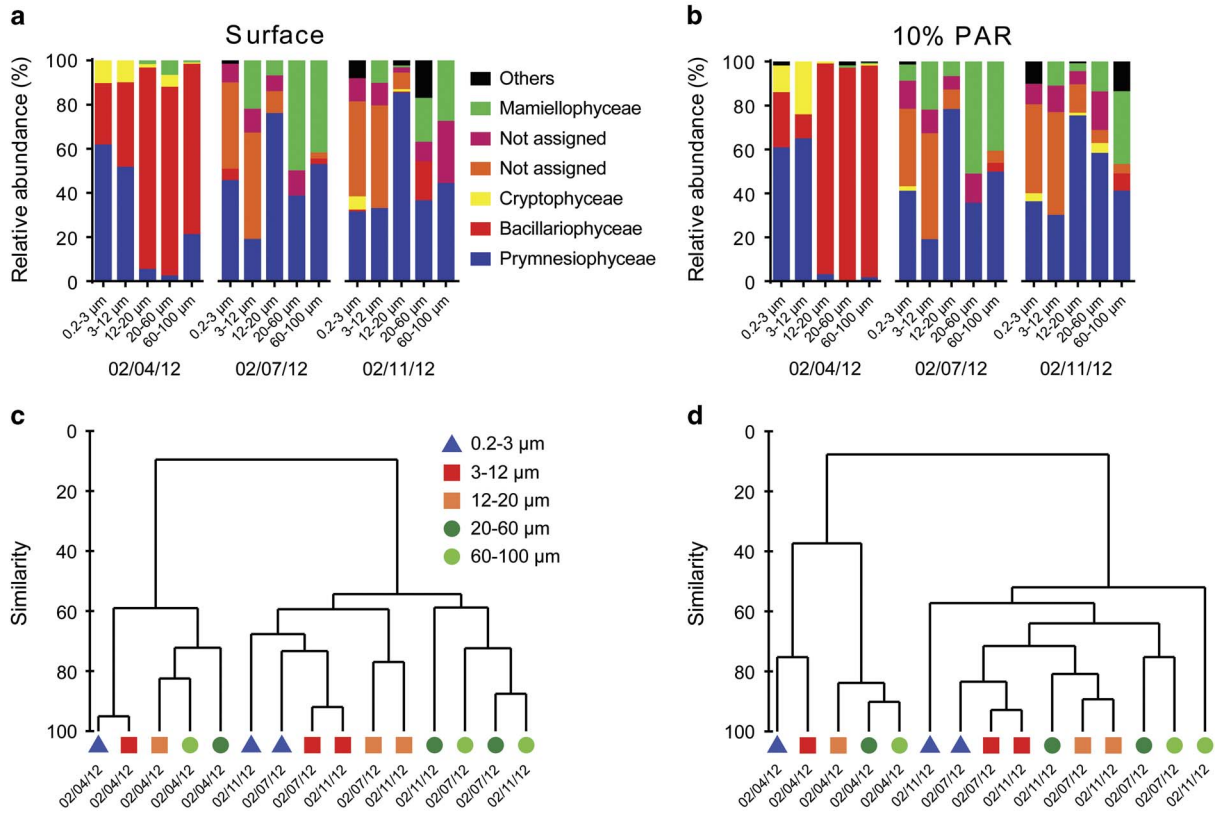

Fig. 5. Taxonomic distribution of the main phytoplankton groups (**a.** and **b.**) and hierarchical cluster (**c.** and **d.**) as determined from T-RFLP$_{HaeIII}$ profiles of the plastid 16S rRNA gene. Bars represent the relative abundance of terminal-restriction fragments (T-RFs) belonging to a given class. 'Others' corresponds to T-RFs < 5% of relative abundance. Size fraction was used as factor for Bray–Curtis similarity analyses. **a.** and **c.** = surface samples, **b.** and **d.** = 10% photosynthetic active radiation (PAR) samples.

of relative abundances (Table III and Table S2): 427, 245, 252, 434, 440 and 836. *In silico* restriction analysis using the PhytoREF plastidial 16S rRNA gene database enabled the identification of four of these six T-RFs (Table III). Taxonomic identification was achieved at the class level for three of the identified T-RFs (T-RFs 252, 434 and 440) and order level for T-RF 836 (Table III). As T-RF 252 matched several plastidial 16S rRNA sequences from different cryptophytes species, *Teleaulax acuta* (Butcher) Hill and *Geminigera cryophila* (Taylor & Lee) Hill (family Geminigeraceae, order Pyrenomonadales), *Pyrenomonas salina* (Wislouch) Santore (family Pyrenomonadaceae, order Pyrenomonadales), and *Cryptomonas curvata* Ehrenberg and *C. paramecium* (Ehrenberg) Hoef-Emden & Melkonian (family Cryptomonadaceae, order Cryptomonadales), it could only be assigned at the class level (Cryptophyceae). Since T-RF 434 corresponded to *Phaeocystis antarctica* Karsten (family Phaeocystaceae, order Phaeocystales) and *Emiliania huxleyi* (Lohmann) Hay & Mohler (family Noelaerhabaceae, order Isochrysidales) it was also assigned at the class level (Prymnesiophyceae). As T-RF 440 corresponded to *Thalassiosira antarctica* Comber, *T. punctigera* (Castracane) Hasle and *Minidiscus trioculatus* (Taylor) Hasle (family Thalassiosiraceae, order Thalassiosirales), but also to *Skeletonema costatum* (Greville) Cleve (family Skeletonemataceae, order Thalassiosirales) and *Phaeodactylum tricornutum* Bohlin (family Phaeodactylaceae) it was assigned as Bacillariophyceae. Since T-RF 836 matched *Ostreococcus lucimarinus* Palenik *et al.* and *Bathycoccus prasinos* Eikrem & Throndsen (family Bathycoccaceae) but also *Mantoniella squamata* (Manton & Parke) Desikachary (family Mamiellaceae) it could be assigned to the order Mamiellales (class Mamiellophyceae). Neither T-RF 245 nor T-RF 427 corresponded to any sequence available for photosynthetic eukaryotes, or even cyanobacteria. These two RFs may correspond to species for which no plastid 16S rRNA sequence is available in public databases. Taxonomic assignment was corroborated using the T-RFs obtained with *Rsa*I (see Table III).

Analysis of the main T-RFs indicates a transition in taxonomic composition of size fractionated phytoplankton through time (Fig. 5a & b). On 4 February, phytoplankton was dominated by Prymnesiophyceae and Bacillariophyceae, while on the following days (7 and 11

https://doi.org/10.1017/S0954102016000699 Published online by Cambridge University Press

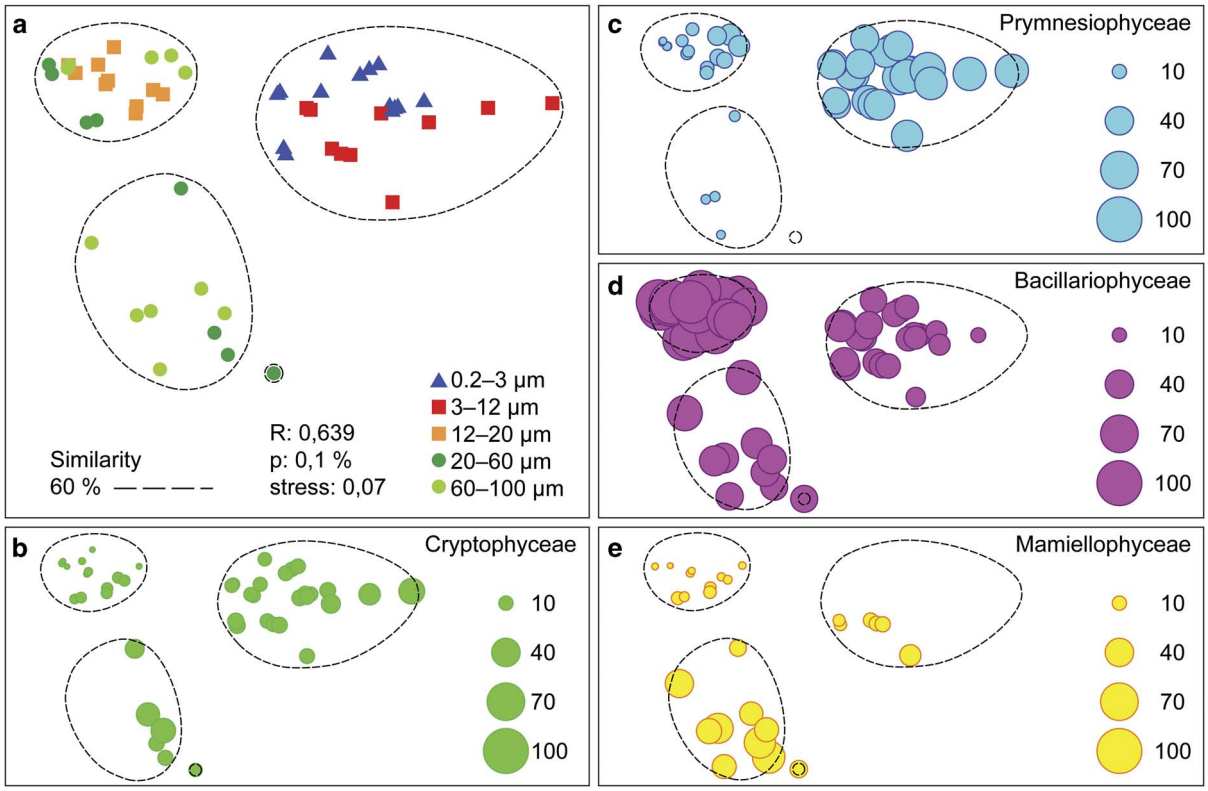

Fig. 6. Non-metric multidimensional scaling analysis of T-RFLP$_{HaeIII}$ profiles of the plastid 16S rRNA gene during summer 2012. **a.** Sample grouping was performed according to size fraction and dotted circles represent > 60% similarity between samples, based on hierarchical cluster analysis of the terminal-restriction fragment length polymorphism (T-RFLP) data. *R* value corresponds to ANOSIM test between size fractions groups. **b.**–**e.** Relative abundance of the main terminal-restriction fragments (T-RFs) that contribute to the difference between photosynthetic eukaryote size fractions. The relative abundance of a given T-RF is indicated by the size of the circle. **b.** = T-RF 252, Cryptophyceae, **c.** = T-RF 434, Prymnesiophyceae, **d.** = T-RF 440, Bacillariophyceae and **e.** = T-RF 836, Mamiellophyceae.

February) Bacillariophyceae were practically absent. During these days, T-RF 427 (not assigned) and Mamiellales showed an increase in relative abundance. Cryptophyceae were detected at the beginning of the sampling period, with predominance in the 0.2–3 µm and 3–12 µm size fractions. At the surface, Cryptophyceae were detected only on 11 February, despite been present in all surface samples analysed by flow cytometry (Fig. 3b).

Hierarchical cluster analyses based on Bray–Curtis dissimilarities of the T-RFLP$_{HaeIII}$ profiles clearly differentiated samples (< 20% similarity) into two main groups based on sampling date (Fig. 5c & d). This differentiation was supported by ANOSIM analysis ($R = 0.639$, $P = 0.1\%$). In addition, SIMPER analysis indicates that four T-RFs were responsible for similarities: 252 (Cryptophyceae), 434 (Prymnesiophyceae), 440 (Bacillariophyceae) and 832 (Mamiellophyceae). Moreover, inside each cluster, samples differentiated between size fractions.

Relative contributions of the T-RFs responsible for the differences observed between size fractions were visualized by NMDS (Fig. 6). Based on this analysis, Prymnesiophyceae and Cryptophyceae were dominant in the 0.2–3 µm and 3–12 µm size fractions (Fig. 6a & b), Bacillariophyceae in the 12–20 µm and 20–60 µm size fractions (Fig. 6d) and Mamiellophyceae were mainly present in the microphytoplankton size fractions (20–60 µm and 60–100 µm) (Fig. 6e). Similar results were obtained after *in silico* assignment of the *Rsa*I T-RFLP profiles (Table III and Tables S2 & S3).

Discussion

Size fractionation of chl *a*, microscopy, flow cytometry and T-RFLP of plastidial 16S rRNA gene analyses were combined to follow the short timescale dynamics of phytoplankton abundance and composition in Fildes Bay, WAP, for 12 days in February 2012. In this study, the hypothesis that Antarctic phytoplankton experiences prompt changes in response to water column conditions during short timescales was tested.

While nutrients are drivers of the phytoplankton composition in many oceanic waters, shallow coastal Antarctic waters are rarely nutrient limited (Agawin *et al.*

https://doi.org/10.1017/S0954102016000699 Published online by Cambridge University Press

2002). In the case of Fildes Bay, reported concentrations are of the order of 2 µM for PO_4^{-3}, 0.2 µM for NO_2^-, 30 µM for NO_3, 80 µM for SiO_3 and 1.5 µM for NH_4 (Lee *et al*. 2015, Luo *et al*. 2015), far from being considered as limiting. In contrast, phytoplankton in Antarctic waters is strongly influenced by the stability of the water column (Garibotti *et al*. 2005, Piquet *et al*. 2011, Marañon *et al*. 2012, Smith *et al*. 2014). Indeed, our results show that Antarctic coastal phytoplankton responds rapidly to changes in the water column stability. Phytoplankton responses to water column stability have been clearly observed over the long term along the WAP (Montes-Hugo *et al*. 2009, Gonçalves-Araujo *et al*. 2015), but few data exist for short timescales (Garibotti *et al*. 2003, Moreno-Pino *et al*. 2016).

Values for seawater physicochemical parameters were consistent with previous reports for the same time of the year in Fildes Bay (Chang *et al*. 1990, Schloss *et al*. 2012, Lee *et al*. 2015). At the beginning of the sampling period, the water column was stratified (Fig. 2) with low chl *a* concentration (Fig. 3a) and low phytoplankton abundance ($< 1 \times 10^3$ cell ml^{-1}; Fig. 3b). As the stability of the water column decreased (7–11 February; Fig. 2), both chl *a* levels and phytoplankton abundance started to increase, with a clear dominance of the nano-sized fraction until the end of the sampling period (Fig. 3). After 11 February, the water column tended to stratify again with a marked increase in both chl *a* and cellular abundances, particularly from the PNE group. Warmer surface waters lasted until the last day of sampling when the water column mixed again, showing the highest biomass, as measured by chl *a* and cell numbers. However, the lack of data from 8–10 February prevents further interpretation of the development of the vertical structure disturbance of the water column.

Phytoplankton composition changed through time in response to water column stability (Fig. 5a & b). At the beginning of the sampling period, the phytoplankton, which was in low abundance, was dominated by Prymnesiophyceae (< 12 µm size fraction) and Bacillariophyceae (> 12 µm size fraction). After the mixing event, taxonomic composition clearly changed (Fig. 5c & d) with a dominance of diatoms (*Thalassiosira*) and haptophytes (*Phaeocystis*), followed by cryptophytes and chlorophytes. *Phaeocystis* (class Prymnesiophyceae) was probably represented by both single-celled and colonial forms, as evidenced by T-RFLP results. The T-RFs assigned to *Phaeocystis* were detected as abundant in the 3–12 µm and 60–100 µm size fractions (Fig. 6c).

Diatoms identified by both microscopy and molecular techniques were similar to those previously identified in coastal Antarctic waters (Mendes *et al*. 2013, Schloss *et al*. 2014, Pearson *et al*. 2015). They were dominant in the > 12 µm size fraction (Fig. 6d & Table II), with both molecular and microscopy data being highly concordant. However, the low taxonomic resolution obtained with T-RFLP assignment did not allow precise determination of diatom taxonomic identity at the species level. Diatom abundance was very low at the beginning (Table II), in concordance with chl *a* data (Fig. 3a). While diatoms other than *Thalassiosira* and dinoflagellates dominated the microplanktonic compartment at the beginning of the sampling (Table II), i.e. when water column was stratified, a strong change in composition was evident after the mixing event occurred (Fig. 5a & b). By 13 February, a strong increase in *Thalassiosira* sp. abundance was observed (Table II), suggesting that this taxon was responsible for the increase in total chl *a* that day (Fig. 3a). An increase in *Thalassiosira* after mixing events has been observed previously in other Antarctic regions (Mendes *et al*. 2013).

Among Prymnesiophyceae (Haptophyta), although it also matches *Emiliania*, the T-RF obtained probably corresponds to *Phaeocystis* since other studies have shown that this genus is abundant in this region (Luo *et al*. 2015, Moreno-Pino *et al*. 2016). Prymnesiophyceae sequences were dominant both in the 0.2–3 µm and 3–12 µm size fractions at the beginning of the sampling period (Fig. 5c & d, Tables II & III and Tables S1–S3). Later, it was detected in both the 3–12 µm and 60–100 µm size fractions (Fig. 6c). The change between the unicellular and colonial life stages of *Phaeocystis* (Whipple *et al*. 2005) could easily explain the dominance of this organism in the nano- and microplankton fraction at different times and the observed increase in PNE abundance during the study (Fig. 3b). As water column mixing developed, Prymnesiophyceae was one of the dominant phytoplankton groups for the rest of the sampling period. Taken together, it is likely that *Phaeocystis* and *Thalassiosira* were responsible for the observed increase in chl *a* (Fig. 3). Arrigo *et al*. (2000) showed that *P. antarctica* dominates during spring in the Ross Sea when the water column is mixed and that their dominance is explained by their ability to photosynthesize under the reduced spring irradiances (Kropuenske *et al*. 2009) allowing them to out compete diatoms. This general pattern was also evidenced at a short timescale in Fildes Bay. However, comparisons, even when attractive, need to be interpreted with caution as these systems present different characteristics. More importantly, in this case timescales are indeed difficult to compare, as long-term data series aiming to understand the ecology and oceanography in Fildes Bay have not been established, in contrast to the Ross Sea (Smith *et al*. 2014).

Cryptophyceae have been previously observed in the study area (Luo *et al*. 2015), as well as in other coastal Antarctic regions (Mendes *et al*. 2013). The T-RF signature did not allow more precise assignment to either Pyrenomonadales (*Geminigera*) or Cryptomonadales (*Cryptomonas*). However, other molecular surveys have

detected *Geminigera* as the dominant cryptophyte in Fildes Bay (Luo *et al*. 2015). Cryptophytes showed low abundance during the sampling period, both in terms of cellular numbers and T-RF abundance, suggesting that they had little influence on chl *a* through the study period (see Figs 3b, 5a, 5b & 6); these findings are in agreement with pigment and microscopy studies that have shown that this group is rarely abundant (Marchant 1993, Garibotti *et al*. 2003).

Mamiellophyceae also contributed to the phytoplankton and were present in low abundances at the beginning of the sampling period, showing an increase after 7 February, as indicated by T-RFLP analysis (Fig. 5a & b). Surprisingly, the T-RF corresponding to Mamiellophyceae was most abundant in the $>12\,\mu m$ size fraction. However, Mamiellophyceae are normally very small, e.g. *Bathycoccus* and *Micromonas* are $<2\,\mu m$ (Vaulot *et al*. 2008). There are a number of possible explanations for their presence in a larger size fraction. The filters may have been clogged during the filtration process, decreasing the effective pore size so that small cells were retained; however, this appears unlikely since similar procedures have been applied in many studies and Mamiellophyceae are always found in the smaller fraction (e.g. Collado-Fabri *et al*. 2011). Alternatively, small Mamiellophyceae may have been either preyed upon or occurring in symbiosis with larger organisms, as has been observed for other prasinophytes (Cachon & Caram 1979) that are retained by 12 μm filters.

Conclusions

Our approach, although limited in its taxonomic resolution, has established the importance of water column stability for phytoplankton composition, which responded at very short timescales (in the order of a day) to changes in mixed layer depth. In the future, combining microscopy, flow cytometry and high-throughput sequencing using specific markers for phytoplankton should improve the taxonomic resolution of the studies.

Acknowledgements

This work was funded by INACH grants T_16-10 and RG_31-15, and Fondecyt grant #11121554 to NT. Collaboration with France was funded through CNRS International Research Network 'Diversity, Evolution and Biotechnology of Marine Algae' (GDRI No. 0803) and ECOS No. C16B02. The authors thank the logistic support at the scientific station, Professor Julio Escudero, Juan Francisco Santíbañez for his invaluable help during the sample collection, Catharina Alves do Souza and Cristián Vargas for their advice and assistance in the microplankton microscopic identification, and Osvaldo Ulloa for his support with the flow cytometry measurements. The authors also thank the reviewers for their comments on the manuscript.

Author contribution

RDI and NT collected the samples. CE performed the T-RFLP analysis. CHC performed the FCM analysis. ND performed the microscopy. EM performed the hydrology analysis. PL, ALS, RDI, DV and NT performed the data analysis and interpretation. ALS, RDI, DV and NT designed the study and wrote the paper.

Supplemental material

Three supplemental tables will be found at http://dx.doi.org/10.1017/S0954102016000699.

References

Agawin, N.S.R., Agustí, S. & Duarte, C.M. 2002. Abundance of Antarctic picophytoplankton and their response to light and nutrient manipulation. *Aquatic Microbial Ecology*, **29**, 161–172.

Arrigo, K.R., Worthen, D., Schnell, A. & Lizotte, M.P. 1998. Primary production in Southern Ocean waters. *Journal of Geophysical Research - Oceans*, **103**, 10.1029/98JC00930.

Arrigo, K.R., DiTullio, G.R., Dunbar, R.B., Robinson, D.H., VanWoert, M., Worthen, D.L. & Lizotte, M.P. 2000. Phytoplankton taxonomic variability in nutrient utilization and primary production in the Ross Sea. *Journal of Geophysical Research - Oceans*, **105**, 10.1029/1998JC000289.

Baldwin, A.J., Moss, J.A., Pakulski, J.D., Catala, P., Joux, F. & Jeffrey, W.H. 2005. Microbial diversity in a Pacific Ocean transect from the Arctic to Antarctic circles. *Aquatic Microbial Ecology*, **41**, 91–102.

Boyd, P.W., Watson, A.J., Law, C.S., Abraham, E.R., Trull, T., Murdoch, R., Bakker, D.C.E., Bowie, A.R., Buesseler, K.O., Chang, H., Charette, M., Croot, P., Downing, K., Frew, R., Gall, M., Hadfield, M., Hall, J., Harvey, M., Jameson, G., LaRoche, J., Liddicoat, M., Ling, R., Maldonado, M.T., Mckay, R.M., Nodder, S., Pickmere, S., Pridmore, R., Rintoul, S., Safi, K., Sutton, P., Strzepek, R., Tanneberger, K., Turner, S., Waite, A. & Zeldis, J. 2000. A mesoscale phytoplankton bloom in the polar Southern Ocean stimulated by iron fertilization. *Nature*, **407**, 695–702.

Cachon, M. & Caram, B. 1979. A symbiotic green alga, *Pedinomonas symbiotica* sp. nov. (Prasinophyceae), in the radiolarian *Thalassolampe margarodes*. *Phycologia*, **18**, 177–184.

Chang, K.I., Jun, H.K., Park, G.T. & Eo, Y.S. 1990. Oceanographic conditions of Maxwell Bay, King George Island, Antarctica (austral summer 1989). *Korean Journal of Polar Research*, **1**, 27–46.

Clarke, A., Meredith, M.P., Wallace, M.I., Brandon, M.A. & Thomas, D.N. 2008. Seasonal and interannual variability in temperature, chlorophyll and macronutrients in northern Marguerite Bay, Antarctica. *Deep-Sea Research II - Topical Studies in Oceanography*, **55**, 1988–2006.

Collado-Fabbri, S., Vaulot, D. & Ulloa, O. 2011. Structure and seasonal dynamics of the eukaryotic picophytoplankton community in a wind-driven coastal upwelling ecosystem. *Limnology and Oceanography*, **56**, 2334–2346.

Decelle, J., Romac, S., Stern, R.F., Bendif, E.M., Zingone, A., Audic, S., Guiry, M.D., Guillou, L., Tessier, D., Le Gall, F., Gourvil, P., Dos Santos, A.L., Probert, I., Vaulot, D, de Vargas, C. & Christen, R. 2015. PhytoREF: a reference database of the plastidial 16S rRNA gene of photosynthetic

eukaryotes with curated taxonomy. *Molecular Ecology Resources*, **15**, 1435–1445.

Díez, B., Massana, R., Estrada, M. & Pedrós-Alió, C. 2004. Distribution of eukaryotic picoplankton assemblages across hydrographic fronts in the Southern Ocean, studied by denaturing gradient gel electrophoresis. *Limnology and Oceanography*, **49**, 1022–1034.

Fuller, N.J., Campbell, C., Allen, D., Pitt, F.D., Zwirglmaier, K., Le Gall, F., Vaulot, D. & Scanlan, D.J. 2006. Analysis of photosynthetic picoeukaryote diversity at open ocean sites in the Arabian Sea using a PCR biased towards marine algal plastids. *Aquatic Microbial Ecology*, **43**, 79–93.

Garibotti, I.A., Vernet, M. & Ferrario, M.E. 2005. Annually recurrent phytoplanktonic assemblages during summer in the seasonal ice zone west of the Antarctic Peninsula (Southern Ocean). *Deep-Sea Research I - Oceanographic Research Papers*, **52**, 1823–1841.

Garibotti, I.A., Vernet, M., Ferrairo, M.E., Smith, R.C., Ross, R.M. & Quetin, L.B. 2003. Phytoplankton spatial distribution patterns along the western Antarctic Peninsula (Southern Ocean). *Marine Ecology Progress Series*, **261**, 21–39.

Gonçalves-Araujo, R., de Souza, M.S., Tavano, V.M. & García, C. A. 2015. Influence of oceanographic features on spatial and interannual variability of phytoplankton in the Bransfield Strait, Antarctica. *Journal of Marine Systems*, **142**, 1–15.

Hasle, G.R. 1978. The inverted-microscope method. *In* Sournia, A., *ed. Phytoplankton manual. Monographs on oceanographic methodology*. Paris: UNESCO, 10 pp.

Henríquez-Castillo, C., Rodríguez-Marconi, S., Rubio, F., Trefault, N., Andrade, S. & De la Iglesia, R. 2015. Eukaryotic picophytoplankton community response to copper enrichment in a metal-perturbed coastal environment. *Phycological Research*, **63**, 189–196.

Holm-Hansen, O., Lorenzen, C.J., Holmes, R.W. & Strickland, J.D.H. 1965. Fluorometric determination of chlorophyll. *Journal Conseil International pour l'Exploration de la Mer*, **30**, 3–15.

Kropuenske, L.R., Mills, M.M., van Dijken, G.L., Bailey, S., Robinson, D.H., Welschmeyer, N.A. & Arrigo, K.R. 2009. Photophysiology in two major Southern Ocean phytoplankton taxa: photoprotection in *Phaeocystis antarctica* and *Fragilariopsis cylindrus*. *Limnology and Oceanography*, **54**, 10.4319/lo.2009.54.4.1176.

Lee, S.H., Joo, H.M., Joo, H., Kim, B.K., Song, H.J., Jeon, M. & Kang, S.H. 2015. Large contribution of small phytoplankton at Marian Cove, King George Island, Antarctica, based on long-term monitoring from 1996 to 2008. *Polar Biology*, **38**, 207–220.

Luo, W., Li, H.R., Gao, S.Q., Yu, Y., Lin, L. & Zeng, Y.X. 2015. Molecular diversity of microbial eukaryotes in sea water from Fildes Peninsula, King George Island, Antarctica. *Polar Biology*, **39**, 10.1007/s00300-015-1815-8.

Marañón, E., Cermeño, P., Latasa, M. & Tadonléké, R.D. 2012. Temperature, resources, and phytoplankton size structure in the ocean. *Limnology and Oceanography*, **57**, 1266–1278.

Marchant, H.J. 1993. Antarctic marine nanoplankton. *In* Menon, J., *ed. Current topics in botanical research*. Trivandrum: Council of Scientific Integration, 189–201.

Mendes, C.R.B., Tavano, V.M., Leal, M.C., de Souza, M.S., Brotas, V. & García, C.A.E. 2013. Shifts in the dominance between diatoms and cryptophytes during three late summers in the Bransfield Strait (Antarctic Peninsula). *Polar Biology*, **36**, 537–547.

Moline, M.A., Prezelin, B.B. & Schofield, O. 1997. Palmer LTER: stable interannual successional patterns of phytoplankton communities in the coastal waters off Palmer Station, Antarctica. *Antarctic Journal of the United States*, **32**, 151–153.

Montes-Hugo, M.A., Vernet, M., Martinson, D., Smith, R. & Iannuzzi, R. 2008. Variability on phytoplankton size structure in the western Antarctic Peninsula (1997–2006). *Deep-Sea Research II - Topical Studies in Oceanography*, **55**, 2106–2117.

Montes-Hugo, M., Doney, S.C., Ducklow, H.W., Fraser, W., Martinson, D., Stammerjohn, S.E. & Schofield, O. 2009. Recent changes in phytoplankton communities associated with rapid regional climate change along the western Antarctic Peninsula. *Science*, **323**, 1470–1473.

Moreno-Pino, M., De la Iglesia, R., Valdivia, N., Henríquez-Castillo, C., Galán, A., Díez, B. & Trefault, N. 2016. Variation in coastal Antarctic microbial community composition at sub-mesoscale: spatial distance or environmental filtering? *FEMS Microbiology Ecology*, **92**, 10.1093/femsec/fiw088.

Pearson, G.A., Lago-Leston, A., Cánovas, F., Cox, C.J., Verret, F., Lasternas, S., Duarte, C.M., Agustí, S. & Serrão, E.A. 2015. Metatranscriptomes reveal functional variation in diatom communities from the Antarctic Peninsula. *ISME Journal*, **9**, 2275–2289.

Piquet, A.M.T., Bolhuis, H., Meredith, M.P. & Buma, A.G.J. 2011. Shifts in coastal Antarctic marine microbial communities during and after melt water-related surface stratification. *FEMS Microbiology Ecology*, **76**, 413–427.

Piquet, A.M.T., Bolhuis, H., Davidson, A.T., Thomson, P.G. & Buma, A.G.J. 2008. Diversity and dynamics of Antarctic marine microbial eukaryotes under manipulated environmental UV radiation. *FEMS Microbiology Ecology*, **66**, 352–366.

Schloss, I.R., Abele, D., Moreau, S., Demers, S., Bers, A.V., González, O. & Ferreyra, G.A. 2012. Response of phytoplankton dynamics to 19-year (1991–2009) climate trends in Potter Cove (Antarctica). *Journal of Marine Systems*, **92**, 53–66.

Schloss, I.R., Wasilowska, A., Dumont, D., Almandoz, G., Hernando, M.P., Michaud-Tremblay, C.A., Saravia, L., Rzepecki, M., Monien, P., Monien, D., Kopczyńska, E.E., Bers, A.V. & Ferreyra, G.A. 2014. On the phytoplankton bloom in coastal waters of southern King George Island (Antarctica) in January 2010: an exceptional feature. *Limnology and Oceanography*, **59**, 195–210.

Schloss, P.D., Westcott, S.L., Ryabin, T., Hall, J.R., Hartmann, M., Hollister, E.B., Lesniewski, R.A., Oakley, B.B., Parks, D.H., Robinson, C.J., Sahl, J.W., Stres, B., Thallinger, G.G., van Horn, D.J. & Weber, C.F. 2009. Introducing Mothur: open-source, platform-independent, community-supported software for describing and comparing microbial communities. *Applied and Environmental Microbiology*, **75**, 7537–7541.

Smith Jr, W.O., Ainley, D.G., Arrigo, K.R. & Dinniman, M.S. 2014. The oceanography and ecology of the Ross Sea. *Annual Review of Marine Science*, **6**, 10.1146/annurev-marine-010213-135114.

Turner, J., Lu, H., White, I., King, J.C., Phillips, T., Hosking, J.S., Bracegirdle, T.J., Marshall, G.J., Mulvaney, R. & Deb, P. 2016. Absence of 21st century warming on Antarctic Peninsula consistent with natural variability. *Nature*, **535**, 10.1038/nature18645.

Vaulot, D., Eikrem, W., Viprey, M. & Moreau, H. 2008. The diversity of small eukaryotic phytoplankton (< 3 μm) in marine ecosystems. *FEMS Microbiology Reviews*, **32**, 795–820.

Vernet, M., Martinson, D., Iannuzzi, R., Stammerjohn, S., Kozlowski, W., Sines, K., Smith, R. & Garibotti, I. 2008. Primary production within the sea-ice zone west of the Antarctic Peninsula. I Sea ice, summer mixed layer, and irradiance. *Deep-Sea Research II - Topical Studies in Oceanography*, **55**, 2068–2085.

West, N.J., Schönhuber, W.A., Fuller, N.J., Amann, R.I., Rippka, R., Post, A.F. & Scanlan, D.J. 2001. Closely related *Prochlorococcus* genotypes show remarkably different depth distributions in two oceanic regions as revealed by in situ hybridization using 16S rRNA-targeted oligonucleotides. *Microbiology*, **147**, 1731–1744.

Whipple, S.J., Patten, B.C. & Verity, P.G. 2005. Life cycle of the marine alga Phaeocystis: a conceptual model to summarize literature and guide research. *Journal of Marine Systems*, **57**, 83–110.

Wright, S.W., Ishikawa, A., Marchant, H.J., Davidson, A.T., van den Enden, R.L. & Nash, G.V. 2009. Composition and significance of picophytoplankton in Antarctic waters. *Polar Biology*, **32**, 797–808.